

FINITE VOLUME MODELING OF THE SOLIDIFICATION OF AN AXIAL STEEL CAST IMPELLER

Received – Prispjelo: 2013-02-03

Accepted – Prihvaćeno: 2013-09-10

Original Scientific Paper – Izvorni znanstveni rad

In the foundry industry, obtaining the solidification contours in cast geometries are extremely important to know the last location(s) to solidify in order to define the correct feeding path and the number of risers. This paper presents three-dimensional simulation of transient conduction heat transfer within an axial impeller, made of AISI 1016 steel, poured and solidified in chemically bonded mold and core medium, by using FVM technique and ANSYS CFX. Specific heat, density and thermal conductivity of AISI 1016 steel, mold and Core materials are considered as functions of temperatures. In this transient thermal analysis, the convection heat transfer phenomenon is also considered at the outer surfaces of the mold. In order to shorten the run-time, the nonlinear transient analysis has been made for 60°/360° segment of the impeller, core and mold. The solidification contours of the impeller as well as isothermal lines in core and mold have been obtained in 3-D. The cooling curves of different points are also shown in the result section.

Key word: steel casting; heat transfer of casting; solidification; finite volume modeling; impeller; ANSYS

INTRODUCTION

Today, the foundry industry is well aware of the fact that knowing solidification sequence is very important to design risers and their connections. Furthermore, knowing the solidification sequence and contours enables the foundry engineer to improve the manufacturability by modifying the original casting designs which are created by the design engineers who are often not familiar with the solidification and how the design parameters affect the solidification pattern.

The first risering equations based on the amount of contraction upon solidification was developed by taking the well known Chvorinov's rule into consideration and Chvorinov's concept of relative freezing time of the riser and casting [1-10].

In fact, modulus method works best for the casting geometries in which none of the mold materials become saturated with heat such as internal corners, internal cores and concave mold surfaces. Nevertheless, almost all casting parts have such geometric features. Thus, foundry engineers faced with a choice: simple but rough modulus method versus complex but more sophisticated numerical methods. Later, the emphasis has shifted to the use of numerical methods such as Finite Difference Method/Finite Element Method (FDM/FEM).

In the first studies, FDM technique was used to simulate solidifications of simple geometries and then applied this technique to designing and risering castings

[11-13]. Numerical methods provided more sophistication than simple relation derived by Chvorinov. However, these techniques require knowledge of thermo-physical properties of metal and mold materials such as specific heat, density and thermal conductivity. These properties are functions of temperature, composition of metal and the solidification rate.

The uses of numerical techniques have been increased as the thermo-physical properties of metals and mold materials at elevated temperatures were studied by several researchers [14-21]. All thermo-physical properties are temperature dependent and vary with compositions. Thus, today, the most challenging and time consuming parts of the simulations are determination of the thermo-physical properties of the materials which will be used in analysis. Special algorithm was developed to calculate the solidification-related thermo-physical properties for plain carbon and stainless steels [16]. The calculated figures were compared with the experimental results, and good correlation was obtained especially for plain carbon steel [16].

The high cost of foundry experiments and trials under daily production conditions makes it appropriate to use all available methods to simulate and to improve the casting design by small modifications. These methods must provide quick results with reasonable accuracy.

Impellers which are the most critical parts of the centrifugal pumps have great impacts on the pump characteristics: Pressure head and flow. Today's pump design engineers use computational fluid dynamic programs in order to design efficient impellers for the targeted pressure heads and flows. Computational Fluid Dynamics programs provide impeller geometries in or-

M. Copur, M. N. Eruslu, Metallurgical and Materials Engineering Department, Faculty of Chemical and Metallurgical Engineering, Istanbul Technical University, Maslak Istanbul, Turkey

der to balance the pressures of the fluids that flow over two sides of the blades of impellers. Thus, outcomes are often designs for the targeted pressure heads and flows, but far from cases of easy and economic casting process. In the successive works, design engineers and the foundry engineers try to modify the impeller geometries for economic casting without losing the pump characteristics. So, it is extremely important to know how a modification affects on the solidification happens during casting to determine the number of risers and their volumes in order to reach better casting yields, and at the end low cost casting.

It is known that several commercial codes are available in the foundry industry to obtain the solidification pattern. However, these commercial codes are used in the foundry industry by foundry engineers, not by engineers in the R&D departments of the pump manufacturers. Once a 3D model is created for CFX modeling, the same model can be used as the preliminary approach to estimate the solidification pattern. In this study, it was shown that the same model can be used to run analyzes for fluid flow and heat transfer together. This gives the possibility to reduce the model set-up time and also reduces the first investment cost that is very important for mid-sized pump manufacturers.

The object of this article is to simulate the solidification of an axial impeller made of AISI 1016 steel, widely used steel in pump industry, poured into chemically bonded urethane molding sand (coarse) and chemically bonded furan core sand (fine) by using a finite volume package. Even though typically pouring temperature is 1923 K, sometime extra high pouring temperatures are used in order to ensure the proper flow through thin blades. Thus, in this study, high pouring temperatures such as 1973 K and 2023 K are also studied in order to understand the effect of superheat on solidification time of different parts of the impeller, especially in the thin blades. The density, specific heat, thermal conductivity of AISI 1016 steel, mold and core sand were considered as temperature dependent. The natural convection properties of the outer surfaces of the mold were considered as constant.

THEORETICAL BACKGROUND

Thermal governing equation

The analytical solutions for the heat conduction equations were derived for infinite and semi-infinite solid bodies at certain boundary conditions. And, the accurate solutions can be obtained for simple geometries. However, the analytical solutions cannot be used for complex geometries having single or multiple cores and concave/convex contours.

It is identical to the transient energy equation given in the following formula [22].

$$\nabla \cdot (k \nabla T) = \rho \cdot \frac{\partial (c_p T)}{\partial t} \quad (1)$$

Where

ρ is the density,

k is conductivity, and

C_p is temperature dependent specific heat including latent heat of solidification.

Thermophysical properties of AISI 1016 steel

Thermo-physical data of AISI 1016 steel are presented in Figures 1, 2, 3 [16].

Thermophysical properties of mold and core materials

In this study, chemically bonded urethane sand (coarse) for mold and chemically bonded furan sand

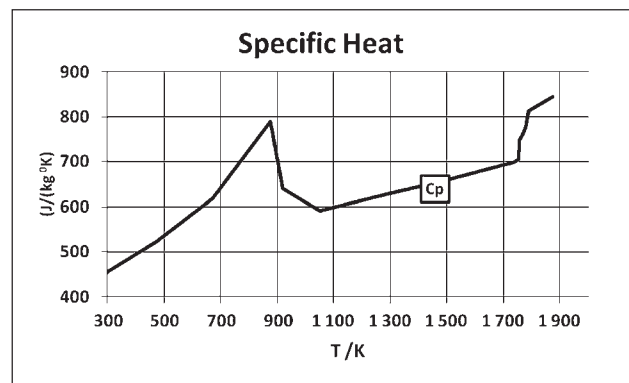


Figure 1 Specific heat graph of AISI 1016 steel versus Temperature [16]

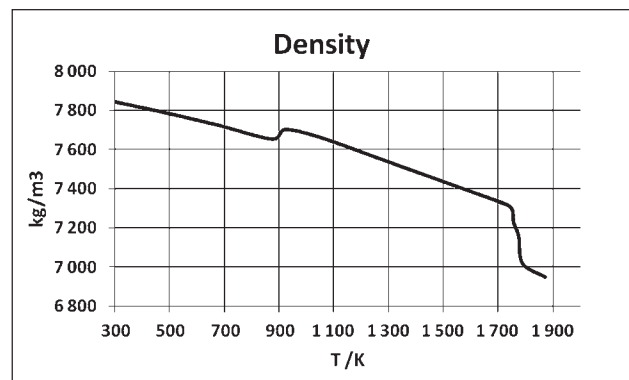


Figure 2 Density of AISI 1016 steel versus temperature [16]

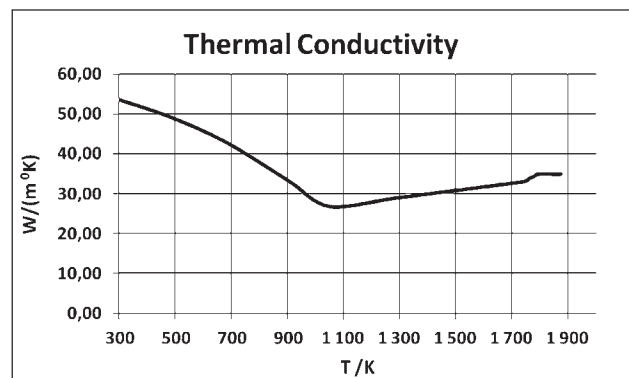


Figure 3 Thermal conductivity of AISI 1016 steel versus temperature [16]

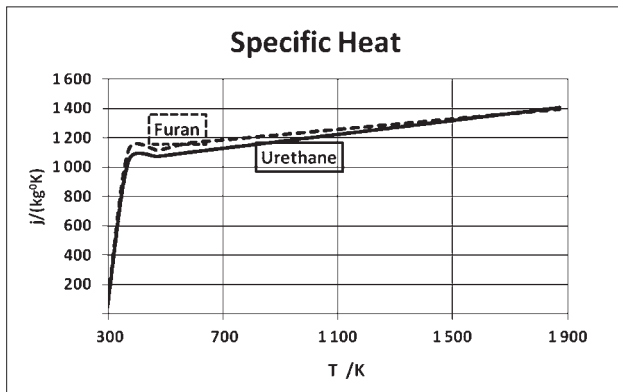


Figure 4 Specific heat of urethane and furan bonded sand versus temperature [23]

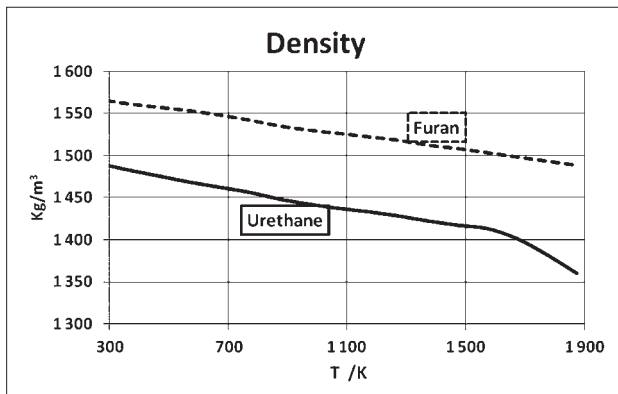


Figure 5 Density of urethane and furan bonded sand versus temperature [23]

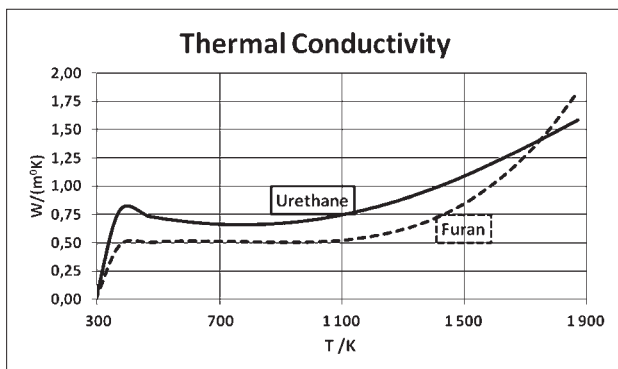


Figure 6 Thermal conductivity of urethane and furan bonded sand versus temperature [23]

(fine) for core have been used. The related thermo-physical data for mold and core materials are presented in Figures 4, 5, 6 [23].

EXPERIMENTAL - MODELING OF THE AXIAL IMPELLER

Methodology

In this study, geometries of impeller and core were designed including the mold medium by using a commercial design program, seen in Figure 7 (Outer radius, height and riser diameter are 300 mm, 172 mm and 150 mm respectively). The geometry was segmented as 60° symmetric parts in Figure 8.

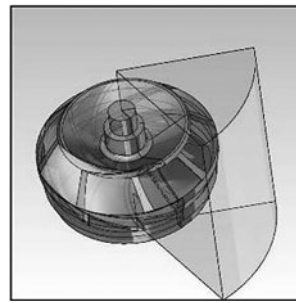


Figure 7 3D drawing of impeller geometry

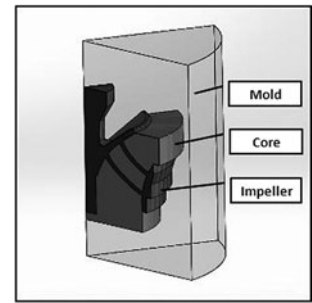


Figure 8 3D model as segmented 60°

In this study, the model impeller geometry has perfect symmetry so it was segmented in order to reduce the number of grids and the run time accordingly. By employing 60° segment model, the number of nodes of the segment has been reduced almost 6 times. After obtaining a solution, 6 segments can be combined to form a complete impeller when analyzing the results by 3-D appearance.

When the geometry is segmented, the initial boundary conditions must be specified that the symmetry is rotational and the symmetry areas are adiabatic.

A CFX program was used to simulate the solidification of AISI 1016 steel in urethane mold and furan core by using a computer of i5 2,9 Ghz and 16 Gb of ram.

Mesh

After the model design was imported into CFX software, an automatic mesh was generated throughout the volume of each domain. In spite of the fact that the automatic mesh provides accurate results for many geometries, because of very complex geometry of the model and high temperature difference between metal/core and metal/mold interfaces, some specific features of software had to be employed to modify the mesh. The options of medium mesh size, Proximity/Curvature and inflation as advanced size functions of mesh were used to generate proper mesh for the model [24-27]. Proximity size function was used to specify a minimum number of element layers created in the regions that constitute gaps in the model such as impeller blades. The proximity was assigned as 3 so that at least 3 layers in cross-sectional dimension of each blade were created. Curvature size feature examines curvature on the edges and faces, and computes element sizes on these entities such that size will not violate the maximum size or the curvature normal angle, which are either computed by the mesher automatically or user-defined. Here in this study, the curvature default was assigned as 0,18 which will enable to simulate a 180° semi-circle curvature as a semi-decagon. Additionally, single body inflation feature was employed in 3-D of impeller body (metal). The inflation feature provides high quality mesh generation close to the wall boundaries to resolve the drastic changes in physical properties. In this study, because of the very high temperature difference at two adjacent grids

on the interfaces of metal/mold and metal/core at initial time ($t = 0$ s), inflation feature was used to reduce the size of mesh elements on the skin of impeller in 3-D. Maximum layer thickness was assigned as 0,4 mm.

After employing these special features of CFX software, the final mesh was generated.

After modification of the mesh by employing mesh size features, mesh statistics was given as 146 962 nodes and 639 981 elements in 60° model segment of impeller mold and core.

Materials and boundary conditions

Specific heat, thermal conductivity and density properties, described in section III and Section IV, as functions of temperature, were inserted as the thermo-physical properties of the impeller (AISI 1016 steel), the mold (Chemically bonded urethane molding sand – coarse) and the core (Chemically bonded furan core sand – fine)

As the initial conditions, at $t = 0$ s, 1 923 K, 1 973 K and 2 023 K were assigned to impeller (metal) for three different solutions. It was 298 K for the mold and the core in all simulations.

The boundary condition is the natural convection generated by the natural aerated environment. For the mold top/bottom surfaces [27] and outer vertical surface [28], 5,75 W/(m²K) and 11,45 W/(m²K) film coefficient values were assigned as the ambient temperature was 298 K.

Transient analysis

Transient type of analysis which employs solution of second order backward Euler equation was used. The convergence of solutions in transient analyzes are the factor that has to be controlled. The CFX software uses a special algorithm to control and to achieve desired convergence criterion. For this, the incremental form of the system equations is solved, the nodal temperature is updated, internal nodal heat flow rates are calculated, the convergence norm (Residual Root-Mean-Square=RMS) is calculated and compared against the criterion. If the norm is equal or smaller than the criterion, no further iteration is needed, and the next time step is performed. In this study, the convergence criterion (Residual RMS) is assigned as 10^{-4} . In order to reach such Residual RMS, the number of iteration, called coefficient loop, in each time step is assigned as 1 for minimum and 15 for maximum.

In this study, 0,5 s for the time step and 7 200 s for the total time were used and, Residual RMS as convergence criterion (10^{-4}) was achieved. The run time for the complete solution was approximately 12 hours

RESULT AND DISCUSSION

The results of this study are mainly the temperature distribution versus time, temperature gradients and cooling curves of points located different place of impeller, core and mold.

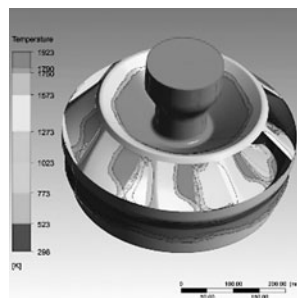


Figure 9 3D impeller at $t = 45$ s ($T_{\text{pouring}} = 1\,923$ K)

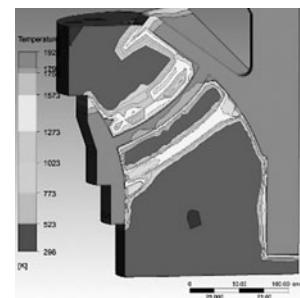


Figure 10 Temperature contours in 60° segment of the impeller and the core at $t = 25$ s ($T_{\text{pouring}} = 1\,923$ K)

After the model is created and simulation is run, it is easy to review the temperature distribution of the impeller as a 60° segment, multiple of segments or in full 3-D appearance, shown in Figure 9.

Additionally, each domain alone or combination of domains may also be easily reviewed. Since the program calculates temperature at all nodes in all domains for all time steps, the review can be done in each incremental time step which had to be defined in the model set-up. In this study, 2,5 s of incremental step was used. It means that the program restores data for the temperature distribution in all domains in every 2,5 s.

The movement of the mushy zone at which hot tear may occur can be reviewed for any time step of solidification.

After the user enters liquidus and solidus temperatures, 1 750 K and 1 790 K respectively, and the time step ($t = t_1$) to the model, the contours of solidus and liquidus temperature are displayed at $t = t_1$.

Figures 10, 11, 12 show the temperature distributions in the impeller and the core at $t = 25$ s, $t = 45$ s and $t = 60$ s respectively for $T_{\text{pouring}} = 1\,923$ K.

As it is seen from the Figure 10, Figure 11 and Figure 12, the liquid portion becomes smaller as the time passes. At the end of 55 s, metal becomes solid. In the meantime, the movement of the mushy zone versus time can also be seen in the Figures.

Similar temperature contours are seen at the author shell for $T_{\text{pouring}} = 1\,923$ K and $T_{\text{pouring}} = 2\,023$ K with 45 s time difference. It is shown in Figure 13.

Depending on the pouring temperature, the complete solidification times of the author shell and hub of impeller is shown in Figure 14.

After a time period of 7 200 s, the simulation is completed. As it is seen in Figure 15 for $T_{\text{pouring}} = 2\,023$ K, even after such a long time, the outer surface of the mold stays approximately at the room temperature. However, after 7 200 s, the inside of the mold including impeller and core have the temperature range between 1 273 K and 1 023 K as the outside of this part have temperature range of 773 K and 523 K. The temperature of the inner parts of the core at early stages of the solidification approaches to the melting temperature of AISI 1016 steel.

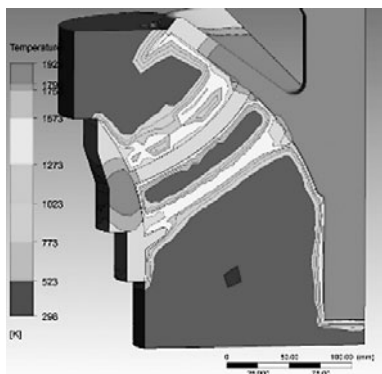


Figure 11 Temperature contours in 60° segment of the impeller and the core at $t = 45$ s ($T_{\text{pouring}} = 1\,923$ K)

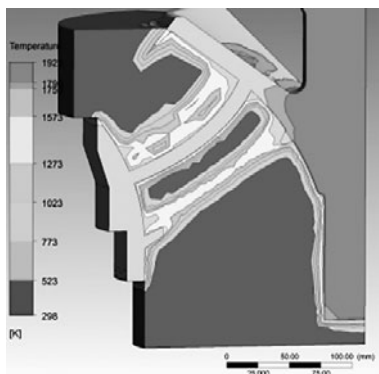


Figure 12 Temperature contours in 60° segment of the impeller and the core at $t = 60$ s ($T_{\text{pouring}} = 1\,923$ K)

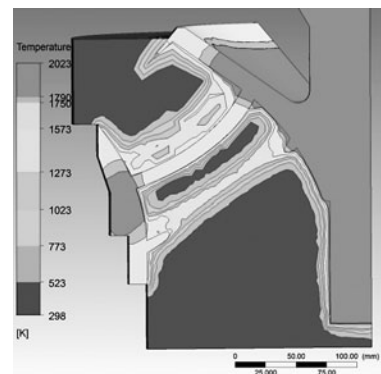


Figure 13 Temperature contours in 60° segment of the impeller and the core at $t = 90$ s ($T_{\text{pouring}} = 2\,023$ K)

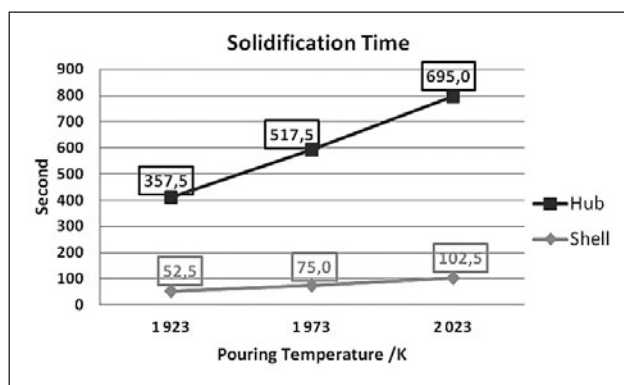


Figure 14 Solidification time calculated at the author shell and the hub

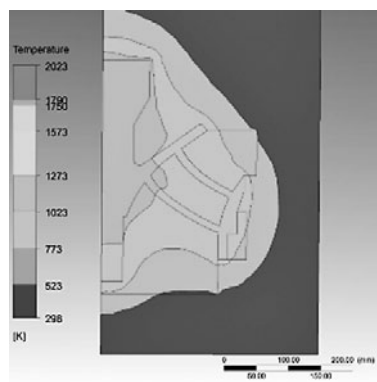


Figure 15 Temperature contours in 60° segment of the impeller, the core and the mold at $t = 7\,200$ s ($T_{\text{pouring}} = 2\,023$ K)

CONCLUSION

In this study, transient heat transfer equations were solved to estimate the solidification sequence of the axial centrifugal pump impeller for different initial conditions by using a Finite Volume Program, Ansys CFX.

The superheat of metal is studied in order to review its effects on the solidification time which changes linearly with superheat. At the lowest pouring temperature (1 923 K) the exterior shell of the impeller solidifies in 35 s. As the superheat goes up to 2 023 K, the solidification time becomes 70 s.

The effect of the mold density, the effect of sand particle size, the use of chill on the solidification time and sequence are also studied, but not presented in this paper.

For the future studies, the researchers can simulate a coupled model of mold filling and subsequent cooling as one model. Researches on different mold filling rates and their effects on the solidification might be the next step of this study.

REFERENCES

- [1] N. Chvorinov, *Giesserei*, 27, 177-186.
- [2] J. B. Caine, *Foundry*, 87 (1963), 120-125.
- [3] C. M. Adams, Jr. and H. F. Taylor, *AFS Transactions*, 61 (1953), 686-693.
- [4] C. M. Adams, Jr. and H. F. Taylor, *AFS Transactions*, 65 (1957), 170-176.
- [5] R. W. Heine, *AFS Transactions*, 76 (1968), 463-469.
- [6] R. Roberts, C. R. Loper, Jr. and R. W. Heine, *AFS Transactions*, 77 (1969), 373-377.
- [7] R. M. Kotschi and C. R. Loper, Jr., *AFS Transactions*, 82 (1974), 535-542.
- [8] C. R. Loper, Jr., *AFS Transactions*, 83 (1975), 173-184.
- [9] R. M. Kotschi and C. R. Loper, Jr., *AFS Transactions*, 84 (1976), 631-640.
- [10] R. M. Kotschi and C. R. Loper, Jr. and M. Copur, *AFS Conference*, 1986.
- [11] A. Jeyarajan and R. D. Pehlke, *AFS Transactions*, 83 (1975), 405-412.
- [12] A. Jeyarajan and R. D. Pehlke, *AFS Monograph*, 1976.
- [13] A. Jeyarajan and R. D. Pehlke, *AFS Transactions*, 86 (1978), 457-463.
- [14] K. Harste: *PhD Dissertation Thesis*, 1989, Technical University of Clausthal.
- [15] R. D. Pehlke, A. Jeyarajan and H. Wada: *Michigan Univ., Report No. NSFMEA82028*, 1982.
- [16] J. Miettinen, *Metall. Trans. B*, 28B (1997), 281-297.
- [17] Y. Meng and B. G. Thomas, *Metal. Trans. B*, 34B (2003), 685-705.
- [18] A. C. Midea and M. Burns, *International Foundry Research*, 59 (2007), 34-43.
- [19] C. A. Santos, J. M. V. Quaresma and A. Garcia, *Journal Alloys and Compounds*, 319 (2001) 174-186.

- [20] M. J. Peet, H. S. Hassan and K. D. H. Bhadeshia, *International Journal of Heat and Mass Transfer*, 54 (2011), 2602-2608.
- [21] S. I. Bakhtiyarov, R. A. Overfelt and D. Wang, *International Journal of Thermophysics*, 26 (2005), 141-149.
- [22] R. W. Lewis, K. Morgan, H. R. Thomas and K. N. Seetharamu, *The Finite Element Method in Heat Transfer Analysis*, Wiley, Wiley, New York, 1996.
- [23] M. J. Keil, J. Rodriguez and S. N. Ramrattan: *AFS Transactions*, 107 (1999), 71-74.
- [24] *ANSYS Handbook*, Chapter 6, Ansys Inc., Canonsbyrg, USA. 2011.
- [25] *ANSYS Handbook, Fundamental FEA Concepts and Applications*, Ansys Inc., Canonsbyrg, USA, 2011.
- [26] *ANSYS Workbench Tutorial*, Ansys Inc., Canonsbyrg, USA, 2010.
- [27] *ANSYS Thermal Analysis Guide*, Ansys Inc., Canonsbyrg, 2010, USA.
- [28] M. M. Pariona and A. C. Mossi: *J. Of r ge Braz. Soc. Of Mech. Sci. And Eng.*, 27 (2005), 399-406.

Note: The responsible for English language is the Lector from Istanbul Technical University, Istanbul, Turkey